Neuroscience 128 (2004) 239–249

METABOLIC CHOLESTEROL DEPLETION HINDERS CELL-SURFACE TRAFFICKING OF THE NICOTINIC ACETYLCHOLINE RECEPTOR

M. F. PEDICONI, C. E. GALLEGOS, E. B. DE LOS SANTOS AND F. J. BARRANTES*

Instituto de Investigaciones Bioquímicas de Bahía Blanca and UNESCO Chair of Biophysics and Molecular Neurobiology, C.C. 857, B8000FWB Bahía Blanca, Argentina

Abstract —The effects of metabolic inhibition of cholesterol biosynthesis on the trafficking of the nicotinic acetylcholine receptor (AChR) to the cell membrane were studied in living CHO-K1/A5, a Chinese hamster ovary clonal line that heterologously expresses adult $\alpha_2\beta\delta\varepsilon$ mouse AChR. To this end, we submitted CHO-K1/A5 cells to long-term cholesterol deprivation, elicited by Mevinolin, a potent inhibitor of 3-hydroxy-3-methyl-glutaryl-CoA reductase and applied a combination of biochemical, pharmacological and fluorescence microscopy techniques to follow the fate of the AChR. When CHO-K1/A5 cells were grown for 48 h in lipid-deficient medium supplemented with 0.5 μM Mevinolin, total cholesterol was significantly reduced (40%). Concomitantly, the maximum number of binding sites (B_{max}) of the cell-surface AChR for the competitive antagonist α-bungarotoxin was reduced from 647±30 to 352±34 fmol/mg protein, i.e. by 46%. The apparent dissociation constant (Kd_{app}) for α-bungarotoxin of the AChRs remaining at the cell surface was not modified by cholesterol depletion. Similarly, the half-concentration inhibiting the specific binding of the radioligand (IC_{50}) for another competitive antagonist, *d*-tubocurarine, did not differ from that in control cells. The decrease in cell-surface AChR was paralleled by an increase in intracellular AChR levels, which rose from 44±2.1% in control cells to 74±3.3% in Mevinolin-treated cells. When analyzed by wide-field fluorescence microscopy, the fluorescence signal arising from α-bungarotoxin labeled cell-surface AChRs was reduced by approximately 70% in Mevinolin-treated cells. The distribution of intracellular AChR also changed: Alexa^{594}-α-bungarotoxin-labeled AChR exhibited a highly compartmentalized pattern, concentrating at the perinuclear and Golgi-like regions. Temperature-arrest of protein trafficking magnified this effect, emphasizing the Golgi localization of the AChR. Colocalization studies using the transiently expressed fluorescent *trans*-Golgi/*trans*-Golgi network marker pEYFP/human β1,4-galactosyltransferase and the *trans*-Golgi network marker syntaxin 6 provided additional support for the Golgi localization of intracellular AChRs. The low AChR cell-surface expression and the increase in intracellular AChR pools in cholesterol-depleted cells raise the possibility that cholesterol participates in the trafficking of the receptor protein to the plasmalemma and its stability at this surface location.

Key words: cholinergic receptor, receptor–lipid interactions, sterol, lipid domains, Golgi apparatus.

Phospholipids and cholesterol (Chol) are the two key lipids for maintaining the correct functioning of integral membrane proteins at the cell surface. Chol is largely confined to the cell membrane, constituting 90% of total cellular content (Lange and Ramos, 1983). The Chol content of cell membranes is strongly regulated, and cells that divide retain all the enzymes necessary for cholesterogenesis. In humans, 50% or more of total body Chol is derived from de novo synthesis. The microsomal enzyme 3-hydroxy-3-methylglutaryl-coenzyme A reductase (HMG-CoA reductase) constitutes a major rate-limiting step in Chol biosynthesis, thus making this enzyme a target of choice for pharmacological regulation of Chol content. Mevinolin (Mev), the drug used in the present work, is a fungal metabolite isolated and purified from *Aspergillus terrus* that acts as a highly potent inhibitor of this enzyme (Alberts et al., 1980).

At the cellular level, variations in membrane Chol have been shown to cause modifications in some cell-surface enzyme and receptor activities, as in the case of permeability to small water-soluble molecules such as monosaccharides and ions (Yeagle, 1993). In MDCK cells, LDL deprivation affects the intracellular trafficking of a model GPI-anchored protein, leading to reduced surface expression (Hannan and Edidin, 1996). In Golgi membranes, Chol levels play a crucial role in intra-Golgi protein transport, and need to be carefully regulated to maintain the structural and functional organization of the Golgi apparatus for intracellular transport to occur (Stüven et al., 2003). It has been reported that Chol depletion specifically affects the transport of vesicles and causes protein accumulation at perinuclear regions (Keller and Simons, 1998; Hansen et al., 2000; Wang et al., 2000; Stüven et al., 2003).

Chol and certain phospholipids are important in the regulation of the nicotinic acetylcholine receptor (AChR) function (McNamee et al., 1982; Criado et al., 1982; see reviews in Barrantes, 1993, 2003). An increase in receptor-mediated ion influx was observed upon increasing the Chol content in reconstituted phosphatidylserine/phosphatidylethanolamine vesicles (Dalziel et al., 1980; McNamee et al., 1982). These observations may be related to the preferential affinity for Chol exhibited by purified AChR in lipid monolayers (Popot et al., 1978; Schindler, 1982) and

*Corresponding author. Tel: +54-291-486-1201; fax: +54-291-486-1200.
E-mail address: rtfjb1@criba.edu.ar (F. J. Barrantes).

Abbreviations: AChR, nicotinic acetylcholine receptor; BFA, Brefeldin A; B_{max}, maximum number of binding sites; α-BTX, α-bungarotoxin; CHO-K1/A5, Chinese hamster ovary cells expressing nicotinic acetylcholine receptor; Chol, cholesterol; *d*-TC, *d*-tubocurarine; ER, endoplasmic reticulum; HMG-CoA reductase, hydroxymethyl-glutaryl CoA reductase; Kd_{app}, apparent dissociation constant; Mev, Mevinolin; pEYFP-Golgi, pEYFP-Gal-T, enhanced yellow fluorescent protein/human β1,4-galactosyltransferase; SM, sphingomyelin; TGN, *trans*-Golgi network.

0306-4522/04$30.00+0.00 © 2004 IBRO. Published by Elsevier Ltd. All rights reserved.
doi:10.1016/j.neuroscience.2004.06.007

bilayer systems (Ellena et al., 1983). Chol has also been reported to be necessary for maintaining the appropriate cohesive pressure required by the AChR to function in a bilayer (Schindler, 1982). In addition, Chol is essential for the preservation of agonist-induced fluxes (Dalziel et al., 1980) and agonist-induced affinity transitions (Criado et al., 1982). Early studies demonstrated that AChR in native *Torpedo* membrane fragments exhibited selectivity for the spin-labeled sterol derivatives androstane and cholestane (Marsh and Barrantes, 1978; Marsh et al., 1981). Labeling and tryptic digestion studies demonstrated that the α-M1, αM4 and γM4 segments interact with Chol (Corbin et al., 1998); photoaffinity sterol reagents like the promegestin promegestone label the AChR transmembrane domain (Blanton et al., 1999); and purified AChR transmembrane segments αM1, αM4, γM1 and γM4 reconstituted in asolectin, display affinities for two sterols, cholestane and androstane, similar to those of the whole AChR (Barrantes et al., 2000).

In addition to these molecular interactions, the AChR protein and Chol have also been reported to interact at the cellular level. Brusés et al. (2001) concluded that Chol was necessary for the maintenance of the neuronal α7-nicotinic AChR in somatic spines of ciliary neurons. Here we investigated whether Chol influences the cell-surface trafficking of the AChR in a model non-neural cell line that stably expresses the adult-type muscle AChR. Chinese hamster ovary cells expressing nicotinic acetylcholine receptor (CHO-K1/A5), a cell line developed in our laboratory that heterologously expresses adult ($\alpha_2\beta\delta\varepsilon$) mouse AChR (Roccamo et al., 1999) was used to test the effect of chronic Chol deprivation induced by Mev. The culture of cells in a lipid-depleted medium containing 0.5 μM Mev for 48 h effectively decreased Chol levels. We studied ligand binding, AChR distribution, metabolic stability, and some pharmacological properties of the AChR in this cell line using the specific non-competitive antagonists [^{125}I]-α-bungarotoxin and *d*-tubocurarine. We found no major changes in the pharmacological properties of the AChR in Chol-depleted cells, but did observe a marked decrease in the proportion of receptor protein present at the cell-surface concomitant with an increase in the intracellular receptor levels. Fluorescence microscopy experiments showed a marked diminution of cell-surface AChR in Chol-depleted cells and a significant accumulation of intracellular receptor in the Golgi apparatus, in particular in the *trans*-Golgi and *trans*-Golgi network (TGN) in Chol-depleted cells, thus suggesting the involvement of Chol in the trafficking of AChR to the plasmalemma.

EXPERIMENTAL PROCEDURES

Materials

[^{125}I]-α-bungarotoxin (α-BTX; 120 μCi/μmol) was purchased from New England Nuclear (Boston, MA, USA). Alexa Fluor^{488}-conjugated α-BTX (Alexa Fluor^{488}-α-BTX) and Alexa Fluor^{594}–α-BTX were from Molecular Probes, OR, USA. α-BTX, *d*-tubocurarine (*d*-TC) and carbamoylcholine were from Sigma Chemical Co. (St. Louis, MO, USA). The enhanced yellow fluorescent protein/human β1,4-galactosyltransferase (pEYFP-Golgi) vector (Clontech Laboratories, Inc., Palo Alto, CA, USA) was a kind gift from Dr. Jennifer Lippincott-Schwartz and Dr. George Patterson, NICHHD, Bethesda, MD, USA. Lipofectin Reagent was from Gibco BRL (Life Technologies, Bs. As., Argentina). The monoclonal mouse antibody anti-syntaxin 6 (product number: VAM-SV025) was from Stressgen Biotechnologies Corporation, Victoria, BC, Canada. Alexa Fluor^{488} F(ab′)$_2$ fragment of goat anti-mouse IgG was from Molecular Probes. Nutridoma-BO medium with controlled lipid content was purchased from Boehringer, Ingelheim, Germany, and Mev was from Merck, Darmstadt, Germany.

Cell culture under control and Chol-depleted conditions

The clonal cell line CHO-K1/A5, obtained by stable transfection of CHO-K1 cells (Roccamo et al., 1999), was grown in Ham's F-12 medium (GIBCO BRL) supplemented with glutamine (Sigma), 40 μg/ml Gentamicin sulfate (Sigma) and 10% bovine fetal serum (Sigma) in a Heraeus Cytoperm incubator maintained at 37 °C with a 5% CO_2/95% air mixture. The cells were grown in this medium for 3–5 days. For Chol deprivation experiments, complete medium was replaced by Nutridoma-BO when cells reached 60–70% confluence. Nutridoma-BO is a lipid-depleted medium (Hanada et al., 1992) consisting of Ham's F-12 medium supplemented with 1% Nutridoma-SP (Boehringer), 0.1% fetal calf serum, 0.2% bovine serum albumin (fatty acid free; Sigma) and 10 μM sodium oleate (Sigma). Cells were further grown for 48 additional hours under five different conditions: a) complete medium (Ham's F-12+10% bovine fetal serum), b) complete medium containing 0.5 μM Mev, c) lipid-depleted medium containing Nutridoma-SP (Nutridoma-BO), d) lipid-depleted medium (Nutridoma-BO) containing 0.5 μM Mev, and e) lipid-depleted medium (Nutridoma-BO) containing 5.0 μM Mev.

Temperature-induced AChR retention at the Golgi apparatus

In order to block protein transport and induce protein retention at the TGN, CHO-K1/A5 cells were incubated at 20 °C for 2.5 h (Xia et al., 1997).

Transfection with pEYFP-Golgi vector

CHO-K1/A5 cells were grown on 25 mm diameter glass coverslips in Ham's F-12 medium for 2 days at 37 °C before being submitted to transient transfection with cDNA coding for the fluorescent Golgi marker pEYFP-Golgi vector using Lipofectin. Twenty-four hours after transfection the complete medium was replaced by Nutridoma-SP, and cells were grown for 48 additional hours with either 0.5 μM or 5.0 μM Mev.

Treatment with Brefeldin A

CHO-K1/A5 cells were grown for 48 h in Nutridoma-BO supplemented with 5.0 μM Mev and further grown with 2.5 μg/ml Brefeldin A (BFA) for 30 min in the continued presence of Mev.

Lipid analysis

Lipid extraction from cell cultures was performed as described by Folch et al. (1957). Briefly, CHO-K1/A5 cells were cultured in 10 cm culture dishes in the presence of complete medium for 5 days, followed by culture in one of the five media described in the preceding section for 48 additional hours. Cells were washed twice with 50 mM HEPES, pH 7.4, scraped from the dishes with a rubber policeman using a small volume of buffer, and transferred to glass tubes. Lipids were extracted with 20 volumes of chloroform: methanol (2:1, v/v) at room temperature for 3 h after dis-

rupting the cells with two 5 s periods using a Branson sonicator. The crude extracts were subsequently centrifuged, partitioned with 0.2 volumes of distilled water and centrifuged again. The lipid-containing organic phase was dried under nitrogen. Samples were resuspended and submitted to thin layer chromatography for the separation of the glycerophospholipids and determination of Chol content. Phospholipid phosphorous was determined from each spot by the method of Rouser et al. (1970), after treatment with perchloric acid at 180 °C. Total Chol content was determined from an aliquot of the total lipid extracts using an enzymatic colorimetric method from Wiener laboratories (Rosario, Argentina). The method is based on the action of Chol hydrolase, Chol oxidase and a peroxidase coupled to a colorimetric assay. Free Chol content was determined by the same colorimetric method in the absence of Chol hydrolase. Chol esters were determined upon subtraction of free Chol from total Chol content.

Equilibrium and kinetic [^{125}I]-α-BTX binding studies

Surface AChR expression was determined by incubating 70–80% confluent cells with increasing concentrations (1–60 nM) of [^{125}I]-α-BTX in cell culture medium for 1 h at 25 °C. At the end of the incubation period, dishes were washed twice with Dulbecco's phosphate-buffered saline, cells were removed by scraping, and collected with 0.1 N NaOH. Radioactivity was measured in a γ counter with an efficiency of 80%. Non-specific binding was determined from the radioactivity remaining in the dishes after initial preincubation of the cells in 10 μM native α-BTX or 2 mM carbamoylcholine chloride before addition of [^{125}I]-α-BTX. Non-specific binding amounted to 10% in control and treated cells.

The metabolic half-life of surface AChR was determined as in Patrick et al. (1977). Cell cultures were labeled with 10 nM [^{125}I]-α-BTX for 1 h at 37 °C, washed twice and incubated for the indicated periods. Non-specific binding was determined as described above for the equilibrium experiments. The half-time of degradation was determined from nonlinear regression analysis of the decay curve corresponding to the radioactivity retained by the cells at different intervals. This followed a mono-exponential time-course. K_{obs} was calculated from linear regression analysis of the kinetics of [^{125}I]-α-BTX association at 10 nM final concentration.

Total AChR was determined after lysis of the cells in 10 mM phosphate buffer, pH 7.4, containing 150 mM NaCl, 5 mM EDTA, 1% Triton X-100, 0.02% NaN_3, 10 μg/ml BSA, 2 mM phenyl methyl sulfonylfluoride, and 10 μg/ml each chymostatin, leupeptin, pepstatin, tosyl-lysine chloromethyl ketone and tosyl phenylalanine chloromethyl ketone, all added to the buffer immediately before use. Cells were lysed overnight at 4 °C (Green and Claudio, 1993) and the binding assay was carried out as described by Schmidt and Raftery (1973). Briefly, 20–40 μl aliquots of the cell lysate were incubated with 10 mM phosphate buffer containing 100 mM NaCl, 1% Triton X-100 and [^{125}I]-α-BTX (60 nM) in a final volume of 125 μl. In these cases, unspecific binding was determined in samples treated 1 h with 2 mM carbamoylcholine chloride, or boiled for 5 min prior to the binding assay. Unspecific binding obtained by either procedure amounted to essentially the same values, approximately 20–30% of the total binding. The binding reaction was terminated by the addition of 100 μl of the incubation reaction to DE-81 paper strips (Whatman; 2×2 cm squares for each sample). DE-81 papers were washed in 10 mM phosphate buffer containing 0.1% Triton X-100 for three 10-min intervals. Dried papers were counted in a Beckman Gamma Counter with 80% efficiency. The intracellular AChR pool was calculated as the difference between total minus cell-surface [^{125}I]-α-BTX binding sites.

Inhibition of initial rates of α-BTX binding

Determination of the IC_{50} for the full antagonist *d*-TC was carried out by measuring the initial rate of [^{125}I]-α-BTX binding after incubation of CHO-K1/A5 cells with *d*-TC. For this purpose, CHO cells were incubated in a reaction volume of 800 μl of culture medium containing the desired *d*-TC concentration for 30 min at room temperature. [^{125}I]-α-BTX was added to the medium to give a final concentration of 10 nM. Cells were incubated in the presence of the iodinated toxin for an additional 20 min. After this period, the medium was removed and cells washed with Dulbecco's buffered saline. Cells were solubilized by the addition of 2 ml of 0.1 N NaOH and the extracts used for radioactivity counting.

Fluorescence microscopy

CHO-K1/A5 cells were grown on 25 mm diameter glass coverslips in Ham's F-12 medium for 2–3 days at 37 °C before cytochemical experiments. For Chol deprivation experiments, complete medium was replaced by Nutridoma-BO and cells were grown for 48 additional hours either in Nutridoma-BO containing 0.5 μM Mev, or in Nutridoma-BO containing 5.0 μM Mev. Control cells were grown in complete medium. Cells were washed twice with PBS. Cell-surface AChR labeling was carried out by incubation of the cells with Alexa Fluor^{488}-conjugated α-BTX (Alexa Fluor^{488}-α-BTX) at a final concentration of 1 μg/ml in PBS, for 1 h, on ice. Excess label was removed by washing with PBS prior to microscopy.

In order to label intracellular AChR, cell-surface AChR were saturated by incubation of CHO-K1/A5 cells with 1 μg/ml α-BTX in PBS for 1 h. Cells were then fixed with 4% paraformaldehyde for 40 min and permeabilized with 0.1% Triton X-100 for 20 min. Finally, cells were incubated with Alexa Fluor^{594}–α-BTX at a final concentration of 1 μg/ml PBS for 1 h.

For colocalization studies of intracellular AChRs with syntaxin 6, immunofluorescence experiments were performed. For this purpose, CHO-K1/A5 cells cultured with 5.0 μM Mev during 48 h, were fixed and permeabilized as described above, and incubated with primary antibody (mouse anti-syntaxin, 1:500) during 1 h at room temperature in PBS containing 1% BSA. Cells were then washed three times with PBS and incubated with secondary fluorophore-conjugated antibody (Alexa Fluor^{488} goat anti-mouse IgG, 1:5000). Alexa Fluor^{594}–α-BTX (final concentration 1 μg/ml in PBS) was added with the secondary antibody to label intracellular AChRs. Incubation was performed at room temperature for 1 h in PBS containing 1% BSA. Cells were washed three times with PBS before coverslips were mounted.

In the recovery experiments, CHO-K1/A5 cells were incubated for 48 h in Nutridoma-BO medium plus 5.0 μM Mev, and subsequently incubated in Ham's F-12 medium supplemented with 10% bovine fetal serum for 24 additional hours. Intracellular AChRs were labeled as described above.

Fluorescence imaging was carried out using a wide-field imaging system (Nikon Eclipse E-600 and TE-300 microscopes). Imaging was accomplished with a SBIG model ST-7 digital charge-coupled device camera (765×510 pixels, 9.0×9.0 μm pixel size; Santa Barbara, CA, USA), with a KXE-2 Apogee 1530×1024 pixel digital charge-coupled device camera (Apogee Systems, Auburn, CA, USA) thermostatically cooled at −10 °C, and a Hamamatsu Orca CCD camera. The ST-7 CCD camera was driven by the CCDOPS software package (SBIG Astronomical Instruments, version 5.02), the KXE-2 CCD was controlled with the PMIS software package version 4.0 (GKRCC Imaging Software, KA) and the Hamamatsu Orca camera was driven by MetaMorph 5.0 software (Universal Imaging Corporation, Downingtown, PA, USA). For all experiments 40× (1.0 NA), 60× (1.4 NA) or 100× (1.4 NA) oil-immersion objectives were used. Appropriate dichroic and emission filters were employed to avoid crossover of fluorescence emission. Background images were

Table 1. Cholesterol and cholesterol esters content in CHO-K1/A5 cells grown under different experimental conditions[a]

Lipid	Complete Ham F-12 medium (5)	Complete medium+Mev (6)	Nutridoma (7)	Nutridoma +Mev (7)
Cholesterol	45±9.5	37±5.3	31±7.0	27±5.4*
Chol esters	22±5.3	13±3.8	17±3.5	13±5.5
Chol esters/Chol	0.48	0.36	0.54	0.49

[a] CHO-K1/A5 cells were grown for 5 days in complete medium (Ham's F-12 plus bovine fetal serum) and then cultured for 48 additional hours under four different experimental conditions (complete medium, complete medium+Mev, Nutridoma BO medium, Nutridoma BO medium+Mev) prior to lipid analysis. Data are expressed as nmol lipid/mg of protein and are the mean±S.D. Figures in parenthesis indicate the number of individual samples analyzed. * $P<0.005$ with respect to control values.

acquired from areas without cells from the same specimen, and subtracted from the cell-containing images. Eight-bit or 16-bit TIFF images were exported for further off-line analysis.

Quantitative fluorescence microscopy analysis

Fluorescence images were analyzed with the software Scion Image version 4.0.2 (Scion Corporation, Frederick, MD, USA). Fluorescence intensities of the eight- or 16-bit images, corrected for background fluorescence, were measured by delimiting the outlines of ROIs. The average fluorescence intensity over distinct areas of the cell surface was calculated for randomly chosen cells for each experimental condition. For illustration purposes, images were processed using Adobe Photoshop 5.5, scaled with identical parameters, and pseudo-colored according to a custom designed look-up-table. In the case of colocalization studies of the receptor with the *trans*-Golgi/TGN marker protein pEYFP-Golgi vector, or with the TGN marker protein syntaxin 6, images were pseudo-colored according to the corresponding emission wavelength of the fluorescent conjugated α-BTX and the specific fluorescent Golgi markers respectively, and analyzed using Scion Image. Deconvolution of images was performed using custom nearest-neighbor and blind deconvolution algorithms.

Protein determination

Total protein content was determined by the method of Lowry et al. (1951) using an aliquot of the cell extracts made with 0.1 N NaOH after radioactivity measurements. Bovine serum albumin was used as standard.

Pharmacological data analysis

Crude data obtained from saturation isotherms, as well as the transformed Scatchard plots, association kinetic constants, ligand-displacement experiments, and half-life of the cell surface AChR were analyzed using the software Origin 6.0. Statistical parameters were determined by the Student's *t*-test (two-tailed).

RESULTS

Changes in lipid content and composition of CHO-K1/A5 cells upon alteration of Chol metabolism

Tables 1 and 2 give the Chol and phospholipid content and the lipid composition of control CHO-K1/A5 cells grown in complete Ham's F-12 medium, and those treated with Mev, a specific inhibitor of HMG-CoA reductase. In control CHO-K1/A5 cells, choline- and ethanolamine-glycerophospholipids are the majority glycerophospholipids (approximately 50% and approximately 25%, respectively), and phosphatidylserine, phosphatidylinositol and sphingomyelin each constitute about 10% of the total (Table 2). No statistically significant variations in glycerophospholipid content were observed in Mev-treated cells (Nutridoma BO+0.5 μM Mev), whereas the free Chol level decreased approximately 40% in Mev-treated CHO-K1/A5 cells with respect to the control condition (CHO-K1/A5 cells grown in complete Ham's F-12 medium). The small pool of Chol esters showed a tendency to diminish upon Mev treatment, but the differences with respect to control cells were not statistically significant (Table 1).

Surface and intracellular levels of [^{125}I]-α-BTX sites

Binding experiments using [^{125}I]-α-BTX were conducted to determine the B_{max} and the Kd_{app} for this competitive antagonist in CHO-K1/A5 cells. Saturation was found between 40 and 60 nM ligand. The B_{max} for the cell-surface AChR obtained from Scatchard analysis was 46% lower in Mev-treated cells (Fig. 1A and Table 3). The diminution of cell-surface AChR induced by Mev was not accompanied

Table 2. Phospholipid content in CHO-K1/A5 cells grown under different experimental conditions[a]

Phospholipid	Complete Ham F-12 medium	Complete medium+Mev	Nutridoma	Nutridoma +Mev
PS	8.7±1.7	7.4±1.6	8.9±1.4	11.6±2.8
PI	7.2±0.6	8.4±0.3	9.0±2.7	8.4±0.6
SM	8.3±2.0	11.0±1.3	11.1±1.5	10.1±0.6
PC	49.8±3.3	46.4±1.4	43.8±2.0	43.5±3.3
PE	26.0±0.1	27.0±1.9	27.2±1.1	26.3±3.5

[a] CHO-K1/A5 cells were grown for 5 days in complete medium (Ham's F-12 plus bovine fetal serum) and then cultured for 48 additional hours under the four experimental conditions listed in the table prior to lipid analysis. Data are expressed as percentages and are the mean±S.D. PC, choline glycerophospholipids; PE, ethanolamine glycerophospholipids; PI, inositol glycerophospholipids; PS, phosphatidylserine.

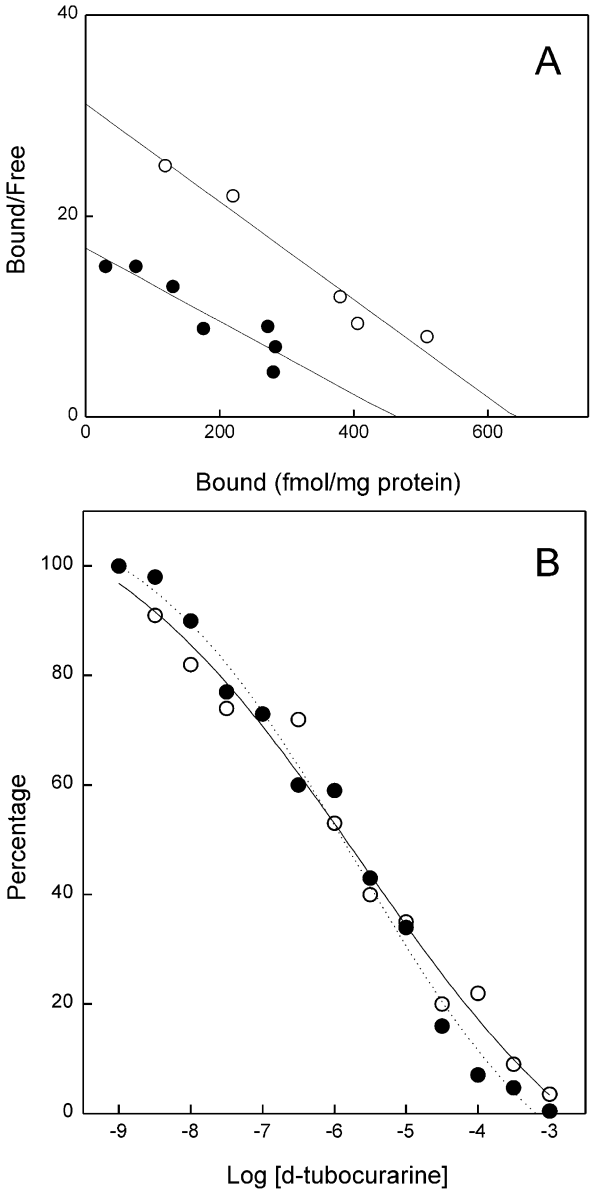

Fig. 1. Scatchard plots (A) and displacement curves (B) of [^{125}I]-α-BTX sites at the cell-surface of CHO-K1/A5 cells grown in complete medium (Ham's F-12 plus bovine fetal serum; ○) or grown for 5 days in complete medium and then in Nutridoma-BO medium (N-BO) with 0.5 μM Mev for 48 additional hours (●). Each point is the mean value of six determinations.

by changes in the affinity for [^{125}I]-α-BTX nor by changes in the total number of sites (Table 3). The intracellular/cell-surface AChR ratio was significantly affected in Chol-depleted cells: 74±3.3% of the AChR remained in intracellular compartments in cells treated with Mev for 48 h in comparison to 44±2.1% of the AChR in intracellular pools in control CHO-K1/A5 cells (Fig. 2).

Kinetics of [^{125}I]-α-BTX binding and ligand-displacement studies

In order to determine whether Chol depletion affected AChR assembly, the kinetics of [^{125}I]-α-BTX association

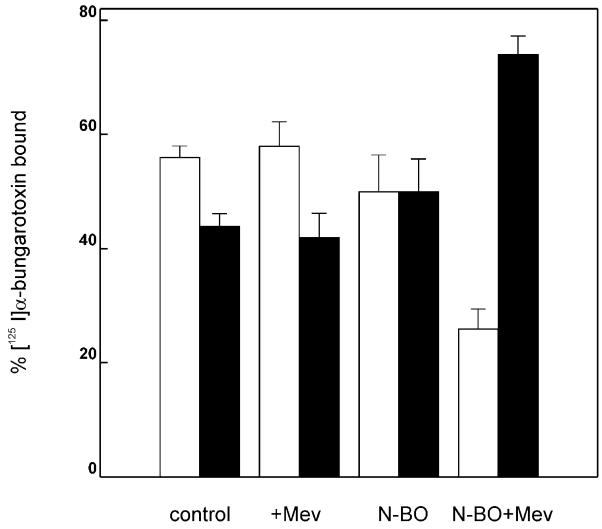

Fig. 2. Proportion of cell-surface and intracellular pools of [^{125}I]-α-BTX binding sites in CHO-K1/A5 cells grown under different culture conditions. Intracellular pools (dark bars) were calculated as the difference between the total minus cell-surface (empty bars) AChR levels in each condition. Data are mean values±S.D. of nine different samples from three separate experiments. Control: CHO-K1/A5 cells grown for 5 days in complete medium (Ham's F-12 plus bovine fetal serum). Other cells were grown as controls and Ham's medium was substituted by the Nutridoma-BO medium (N-BO) with or without 0.5 μM Mev for an additional 48 h.

with cell-surface AChR was studied next. Almost 90% of the radioligand was bound to the AChR within the first hour of the kinetic assay in Mev-treated cells, whereas in control cells only 67% of the maximum binding was accomplished within this period (Roccamo et al., 1999). Linearization of the kinetic curves obtained by plotting ln (Beq/Beq-Bt) as a function of time (Yamanaka et al., 1986) yielded apparent k_{on} values of 1.2±0.12 h^{-1} for control CHO-K1/A5 cells (r=0.92) and 2.81±0.06 h^{-1} for cells grown in Nutridoma-BO medium in the presence of 0.5 μM Mev (r=0.99).

The displacement of [^{125}I]-α-BTX by the competitive antagonist *d*-TC was studied in another series of experiments. The reduction of [^{125}I]-α-BTX binding sites produced by *d*-TC in CHO-K1/A5 cells grown in complete Ham F-12 medium was similar to that of cells grown in Mev-containing Nutridoma medium. Values of IC_{50} of 5.6–5.7 μM were obtained in both conditions (Fig. 1B). Plots of log (b/Bmax-b) as a function of ligand concentration yielded n_H values of 1.20±0.25 and 1.29±0.05 for control and Chol-depleted cells, respectively. From the two sets of experiment we can conclude that the pharmacological response to the two cholinergic antagonists is not modified upon Mev-mediated Chol depletion.

The half-life of the AChR varies among different cells (Gu et al., 1990; Roccamo et al., 1999). Chol depletion by Mev increased the metabolic turnover of the cell-surface AChR: The half-life of the AChR in Mev treated cells was 3.2 h, whereas in control cells $t_{1/2}$ was 4.2 h (data not shown).

Table 3. [^{125}I]-α-BTX binding to CHO-K1/A5 cells grown under different culture conditions[a]

	Complete medium	Complete medium+Mev	Nutridoma	Nutridoma +Mev
Surface [^{125}I]-α-BTX	647±30	595±25	575±40	352±34*
Kd_{app} cell-surface [^{125}I]-α-BTX	26±2.1	15±2.8	19±0.7	23±5.4
Total [^{125}I]-α-BTX	1155±150	1021±176	1171±138	1348±270

[a] CHO-K1/A5 cells were grown for 5 days in complete medium (Ham's F-12 plus bovine fetal serum) and then cultured for 48 additional hours under the four experimental conditions listed in the table prior to the toxin binding assays. Surface and total AChR are expressed as fmol of specifically bound [^{125}I]-α-BTX/mg protein. B_{max} and Kd_{app} were obtained from the transformed Scatchard plots of the saturation isotherms obtained in the presence of [^{125}I]-α-BTX in the 5–60 nM range. Total AChR was determined from solubilized cells as indicated under Experimental Procedures. Results are the mean±S.D. values from three separate experiments. * $P<0.001$ with respect to control values.

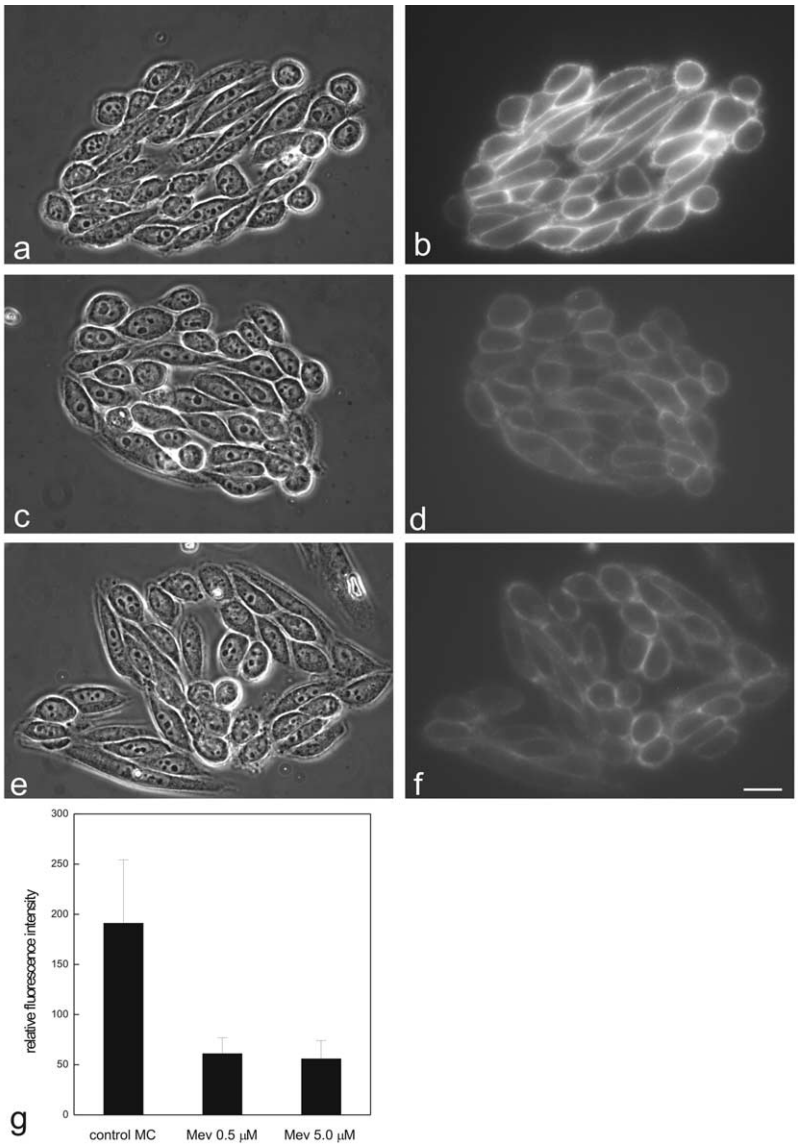

Fig. 3. Cell-surface fluorescence of Alexa Fluor^{488}–α-BTX in CHO-K1 cells treated with Mev. (a, b) Control cells grown in complete medium (Ham's F-12 plus bovine fetal serum). (c, d) CHO-K1/A5 cells treated with 0.5 μM Mev. (e, f) Cells treated with 5 μM Mev. (a), (c) and (e) are phase contrast images, and (b), (d) and (f) the corresponding fluorescence images. (g) Relative distribution of Alexa Fluor^{488}–α-BTX cell-surface fluorescence intensity in CHO-K1/A5 cells treated with Mev at the indicated concentrations. Scale bar=10 μm.

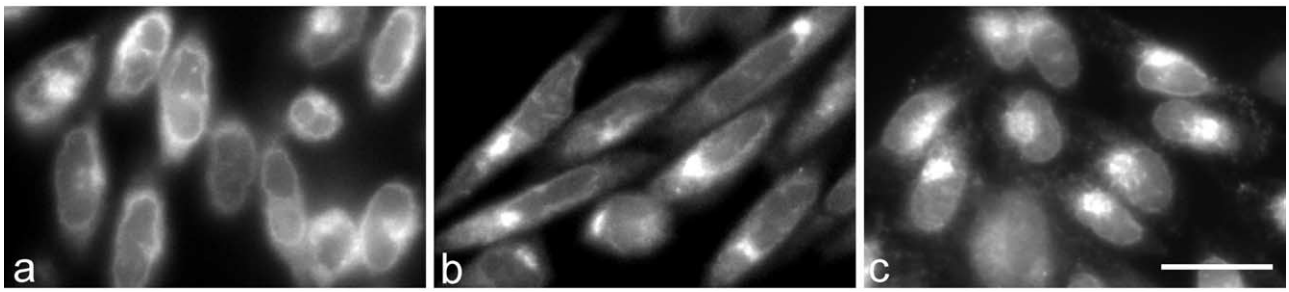

Fig. 4. Fluorescence distribution of intracellular Alexa Fluor^{594}–α-BTX-labeled AChRs. (a) Control CHO-K1/A5 cells grown in complete medium. AChRs are distributed evenly over the entire cell. (b) Inhibition of Chol biosynthesis by 5.0 μM Mev in CHO-K1/A5 cells produced perinuclear and Golgi-like accumulation of AChRs. (c) Block of protein transport and retention in the TGN by temperature arrest (incubation of CHO-K1/A5 cells for 2.5 h at 20 °C as described by Xia et al. (1997) in complete medium). AChR labeled with Alexa Fluor^{594}–α-BTX shows a similar distribution to that observed in Mev-treated cells. Scale bar=10 μm.

Cell-surface distribution of fluorescent-labeled AChR

The fluorescence staining of AChR with a fluorescent derivative of α-BTX, Alexa Fluor^{488}–α-BTX, exhibited a finely punctuate distribution over the entire cell surface of CHO-K1/A5 cells (Fig. 3b). Mev treatment significantly reduced cell-surface fluorescence (Fig. 3d–f). This effect was already apparent at 0.5 μM Mev (Fig. 3d), with >50% reduction of surface receptor-associated specific fluorescence (Fig. 3g). Higher (5.0 μM) Mev concentrations produced essentially the same reduction in cell-surface fluorescence levels (Fig. 3g).

Intracellular distribution of fluorescent-labeled AChR

Fixed, permeabilized CHO-K1/A5 cells exhibited a mostly uniform distribution of Alexa Fluor^{594}–α-BTX fluorescence over the entire cell (Fig. 4a). Mev treatment changed this fluorescence pattern. Fluorescence acquired a more compartmentalized, perinuclear distribution (Fig. 4b), compatible with the accumulation of AChRs at the Golgi region.

In order to define the precise localization of intracellular AChR, the artificial accumulation of receptors was induced by temperature-arrest of transport, i.e. incubation of CHO-K1/A5 cells at 20 °C. This procedure blocks protein trans-

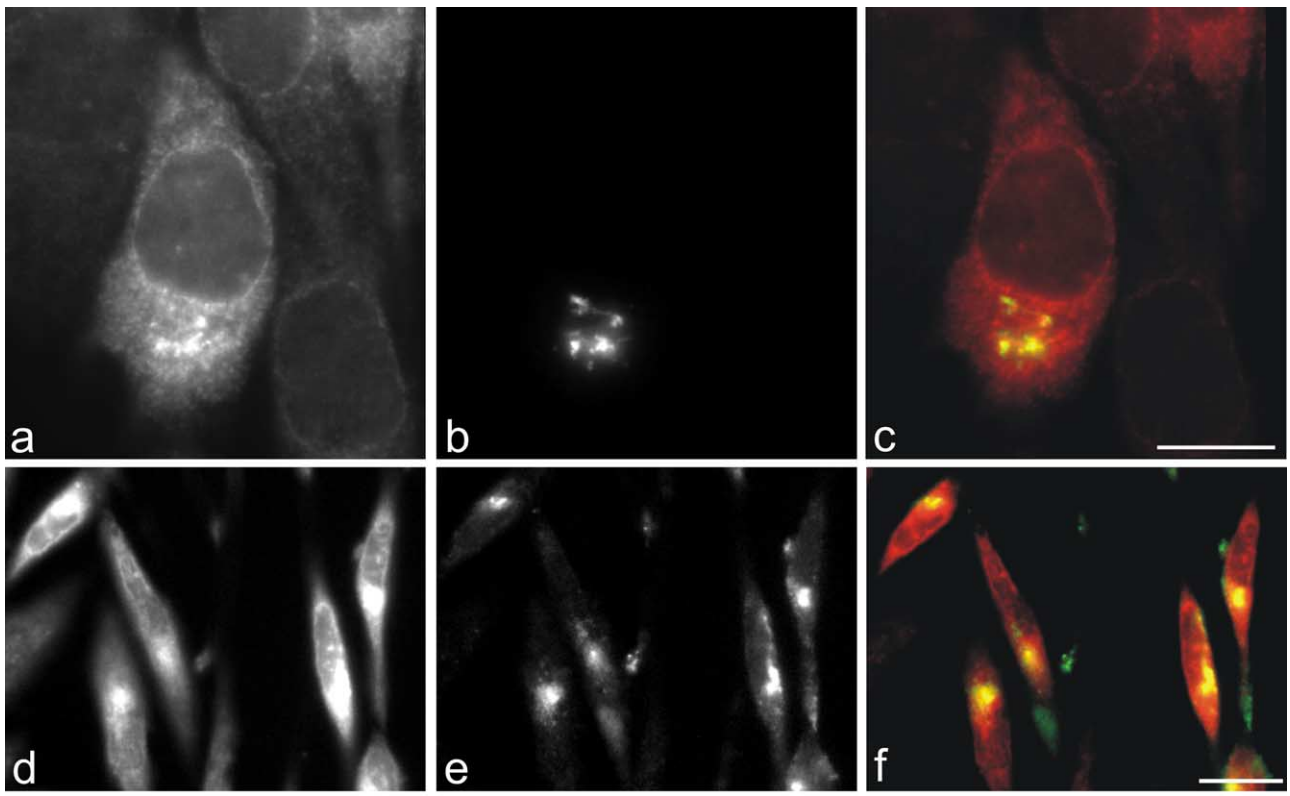

Fig. 5. Colocalization of intracellular AChR with the *trans*-Golgi/TGN and TGN markers pEYFP-Gal-T and syntaxin 6 in 5.0 μM Mev CHO-K1/A5-treated cells. (a) Intracellular AChR labeled with Alexa Fluor^{594}–α-BTX. (b) Fluorescence corresponding to the fusion protein pEYFP-Gal-T. (c) Overlay of images (a) and (b). (d) Intracellular AChR labeled with Alexa Fluor^{594}–α-BTX. (e) Immunofluorescence staining of syntaxin 6. (f) Overlay of images (d) and (e). Scale bar=10 μm.

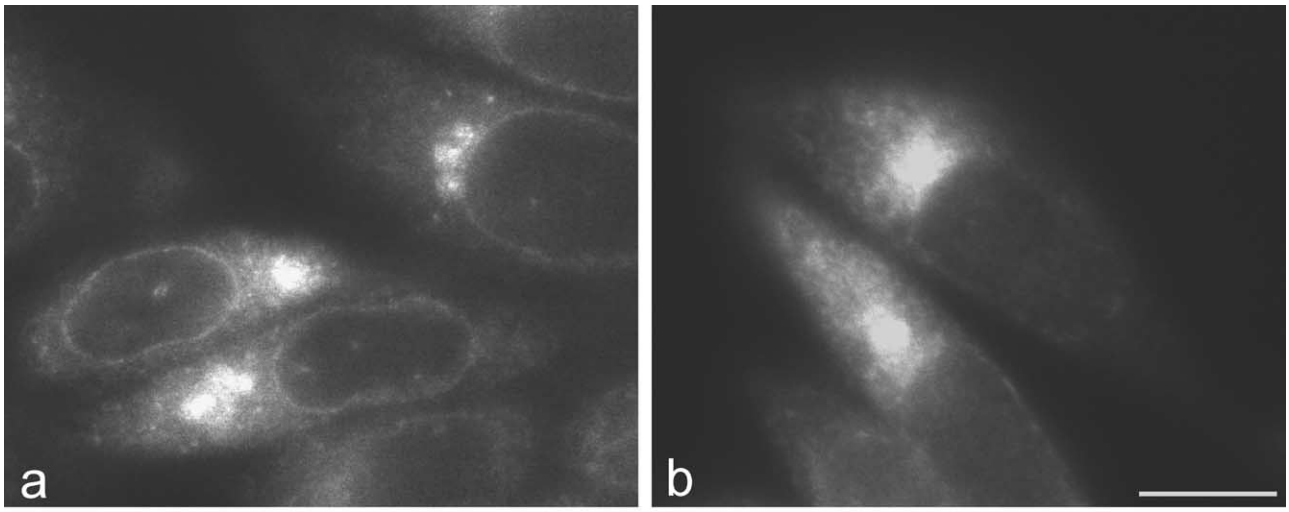

Fig. 6. Deconvoluted images of intracellular Alexa Fluor^{594}–α-BTX-labeled AChR. CHO-K1/A5 cells were grown for 48 h in delipidated Nutridoma-BO medium containing 5.0 μM Mev (a) or further incubated with 2.5 μg/ml BFA for 30 min, in the continued presence of Mev (b). Scale bar=10 μm.

port in CHO-K1 cells, principally at the TGN level (Xia et al., 1997). The fluorescence pattern of the Alexa Fluor^{594}–α-BTX -labeled AChR in the 20 °C protein-arrested cells was very similar to that of intracellular AChR in Mev-treated cells: in both cases fluorescence was associated with a Golgi-like compartment (Fig. 4).

In order to confirm the Golgi localization of AChRs in Chol-depleted cells, the AChR-expressing clone CHO-K1/A5 was transiently transfected with the pEYFP-Golgi vector, which codifies for the pEYFP-Gal-T. Gal-T-GFP colocalizes in HeLa cells with endogenous Gal-T during all stages of the cell cycle (Zaal et al., 1999). The enzyme Gal-T was shown to be localized in *trans*-Golgi cisternae (Roth and Berger, 1982) and the TGN (Lucocq et al., 1989; Nilsson et al., 1993). CHO-K1/A5 cells were treated with Mev as in previous experiments and intracellular AChR was stained with Alexa Fluor^{594}–α-BTX. The most intense Alexa Fluor^{594}–α-BTX fluorescent regions (Fig. 5a) exhibited colocalization with the *trans*-Golgi/TGN marker (Fig. 5c).

In another series of experiments, Chol-depleted CHO-K1/A5 cells were treated with BFA for 30 min in the continued presence of Mev. BFA is a fungal metabolite known to cause the retrograde traffic to the endoplasmic reticulum (ER) of membrane constituents of the *cis*-, *medial*- and *trans*-Golgi, but not the TGN (Lippincott-Schwartz et al., 1991; Rosa et al., 1992; Banting and Ponnambalam, 1997; Chardin and McCormick, 1999; Watson and Pessin, 2000). No changes in the distribution of intracellular AChR fluorescence were observed upon BFA treatment in Mev-treated cells, which remained in a clustered perinuclear location, where the TGN and late endosomes are usually found (Fig. 6). This is a further indication that AChR accumulation occurred at the TGN level.

To confirm the localization of the AChR accumulated intracellularly, immunofluorescence experiments were performed using anti-syntaxin 6 antibody, a specific marker of the TGN compartment (Vandenbulcke et al., 2000). Syntaxin 6 is a member of the syntaxin family, whose constituents are required for several vesicle trafficking pathways. By immunoelectron microscopy, syntaxin 6 was shown to localize primarily at the TGN and small vesicles in the vicinity of endosome-like structures (Bock et al., 1997). Intracellular AChR and syntaxin 6 in CHO-K1/A5 cells treated with 5.0 μM Mev showed a partial overlap of both fluorescent signals (Fig. 5).

When CHO-K1/A5 cells treated with 5.0 μM Mev were subsequently cultured in complete Ham's F-12 medium

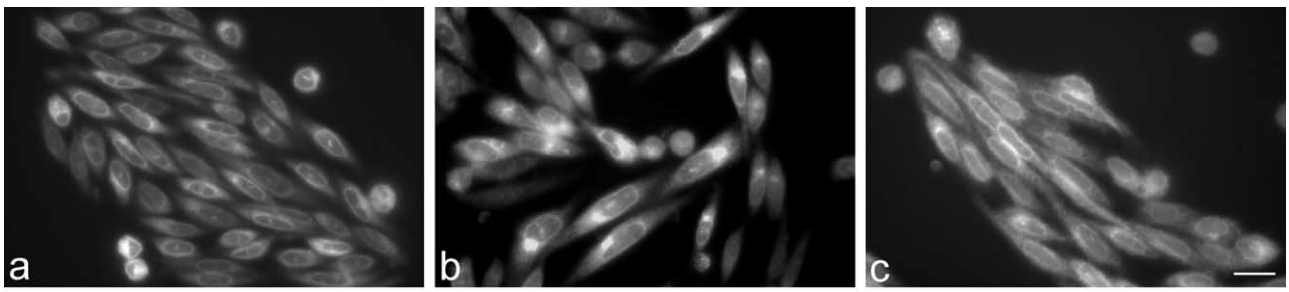

Fig. 7. Intracellular AChR labeled with Alexa Fluor^{594}–α-BTX in control CHO-K1/A5 cells (grown in Ham's F-12 medium plus bovine fetal serum) (a), CHO-K1/A5 cells treated with 5.0 μM Mev for 48 h (b), or cells treated as in (b) and subsequently allowed to recover by incubation in Ham's F-12 medium supplemented with 10% bovine fetal serum for 24 additional hours (c). Scale bar=10 μm.

supplemented with 10% bovine fetal serum for 24 additional hours, the Alexa Fluor^{594}–α-BTX fluorescence pattern observed in control cells was restored (Fig. 7), thus demonstrating the reversibility of the Mev effect.

DISCUSSION

Inhibition of the Chol-synthesizing enzyme HMG-CoA reductase in AChR-producing CHO-K1/A5 cells with the drug Mev resulted in the diminution of cellular Chol levels, decreased the amount of AChR at the cell surface, and increased the amount of AChR retained inside the cell. Variations in the amount of cell-surface AChR in Chol-depleted cells might result from alterations in the synthesis, assembly, internalization, or trafficking of the receptor. The first possibility can be discarded right from the outset, since no differences were found in the *total* amount of AChR measured by [^{125}I]-α-BTX binding between control and Mev-treated cells (Table 3).

A second possibility is that the significant decrease in the amount of the AChR present at the plasmalemma of Mev-treated cells resulted from altered assembly of the five subunits. We detected an approximately 2.5-fold increase in the association kinetics of [^{125}I]-α-BTX to the AChR in Chol-depleted cells. The apparent association rate constant of α-BTX for the complete oligomeric, assembled AChR differs from that of the unassembled α-subunit (Blount and Merlie, 1989). The association kinetics of a cell line expressing only α-subunits has been reported to be faster than that of cells expressing the full dotation of muscle subunits, i.e. $\alpha_2\beta\gamma\delta$ (Blount and Merlie, 1988). However, in the absence of assembly with other subunits, the α-subunit is confined to intracellular compartments and is not transported to the plasma membrane (Blount and Merlie, 1988; Wang et al., 2002). AChR subunits exit the ER only as fully assembled pentamers (Smith et al., 1987; Gu et al., 1989; Ross et al., 1991; Gelman et al., 1995). ER chaperones and specific signals within the AChR subunits act as part of the quality control machinery regulating ER-to-Golgi trafficking and keeping immature proteins in the ER (reviewed in Wanamaker et al., 2003). Additional evidence argues against the possibility of AChR misfolding as a result of Chol depletion: unassembled AChR displays altered displacement curves of small cholinergic ligands such as curare (Blount and Merlie, 1991). No differences were found here in the ability of *d*-TC to displace [^{125}I]-α-BTX binding between control and Mev-treated cells; IC_{50} values for *d*-TC upon Chol depletion did not statistically differ from those of control cells (Fig. 1B). Similarly, equilibrium binding of [^{125}I]-α-BTX to the AChR exhibited affinities typical of the complete AChR oligomer in Mev-treated cells (Table 3).

A third possibility is that the decrease in cell-surface AChR resulted from the impaired stability of newly synthesized receptor molecules at the plasmalemma. If the maintenance of AChR at the cell surface depended on the correct lipid-protein balance at the plasmalemma, variations in cell surface Chol might alter the microarchitecture of the membrane domains where the AChR occurs. Data recently reported by Brusés et al. (2001) is in agreement with this hypothesis: maintenance of the α7 neuronal AChR at the plasma membrane of ciliary neurons is indeed Chol-dependent. Our results show that Chol depletion by Mev accelerated the metabolic turnover of the cell-surface AChR in CHO-K1/A5 cells. The half-life of the AChR in Mev treated cells was shorter than that found in control cells; this third possibility cannot therefore be discarded.

A fourth possibility is that Chol is implicated in AChR trafficking to the plasma membrane. Using a temperature-dependent sphingolipid-deficient clonal CHO cell line, we observed that lower levels of sphingomyelin (SM) adversely affected AChR trafficking to the cell surface, leading us to suggest that SM could be involved in AChR trafficking (Roccamo et al., 1999). More recently, we were able to measure the affinity of the membrane-bound and purified *Torpedo* AChR for a fluorescent SM-derivative; SM exhibits only a moderate affinity for the receptor (Bonini et al., 2002). Chol-SM microdomains or "rafts" are postulated to result from preferential interactions between these two lipid species, giving rise to lateral segregation that facilitates the favored insertion of certain proteins having a sterol-sensing domain (Kurzchalia and Parton, 1999; Smart et al., 1996).

The perinuclear accumulation and clustering of the AChR upon Mev treatment (Fig. 4b), the maintenance of this intracellular distribution after BFA treatment (Fig. 6b), the AChR colocalization with the *trans*-Golgi/TGN and TGN markers pEYFP-Golgi vector and syntaxin 6, respectively (Fig. 5c, f), and the reversibility in the Mev effect (Fig. 7), all indicate that Mev-induced Chol depletion results in receptor accumulation at the *trans*-Golgi/TGN, and suggest the involvement of Chol in receptor trafficking from this organelle to the plasma membrane. Chol levels in Golgi membranes play a crucial role in intra-Golgi protein transport, and the Chol content must be carefully balanced to allow intracellular transport to occur (Stüven et al., 2003).

"Raft" lipid domains also occur at the Golgi complex, and have been shown to serve as platforms in the TGN for sorting in both polarized and nonpolarized cells (Simons and van Meer, 1988; van Meer and Simons, 1988; Simons and Ikonen 1997). Keller and Simons (1998) reported that Chol depletion specifically affects TGN-derived transport vesicles, but has no effect on ER-to-Golgi traffic. Hansen et al. (2000) found that Chol depletion affected membrane trafficking of aminopeptidase N in enterocytes, increasing basolateral missorting of the protein. GPI-anchored proteins (Brown and Rose, 1992) and carboxypeptidase E (Dhanvantari and Loh, 2000; Zhang et al., 2003) become raft-associated during passage through the Golgi apparatus. In agreement with our results, Lovastatin-induced Chol depletion caused the reversible block of secretory granule biogenesis, and accumulation of the secretory protein POMC at the TGN (Wang et al., 2000). Heino et al. (2000) also found that the disassembly of the Golgi complex blocks the transport of both Chol and the influenza virus hemagglutinin, an integral transmembrane protein, to the cell surface. The myristoylated protein rapsyn is co-tar-

geted with the AChR to the postsynaptic membrane via the exocytic pathway (Marchand et al., 2000), and in COS-7 cells, the sorting and trafficking of the two proteins is mediated by association with Chol-sphingolipid-enriched raft microdomains (Marchand et al., 2002). All these findings reinforce the view that Chol may be involved not only in the maintenance of the affinity state transitions at the plasma membrane (Criado et al., 1984; reviewed in Barrantes, 1993) but also in the delivery of newly synthesized AChR to the cell surface, via association with lipid platforms. In conclusion, the decreased cell-surface AChR levels upon Chol depletion appear to result from a) inhibition of AChR trafficking from the Golgi apparatus to the plasma membrane, with the concomitant accumulation of newly synthesized AChRs at the *trans*-Golgi/TGN level; b) the decreased stability of cell-surface AChR upon Chol depletion; or c) a combination of both.

Acknowledgments—This work was supported in part by grants from the Universidad Nacional del Sur, the Agencia Nacional de Promoción Científica (Foncyt), Fundación Antorchas, Argentina, and FIRCA 1-RO3-TW01225-01 to F.J.B. and Universidad Nacional del Sur to M.F.P.

REFERENCES

Alberts AW, Chen J, Kuron G, Hunt V, Huff J, Hoffman C, Rothrock J, Lopez M, Joshua H, Harris E, Patchett A, Monagham R, Currie S, Stapley E, Albers-Shonberg G, Hensens O, Hirshfield J, Hoogsteen K, Liesch J, Springer J (1980) Mevinolin: a highly potent competitive inhibitor of hydroxymethylglutaryl-coenzyme A reductase and a cholesterol lowering agent. Proc Natl Acad Sci USA 77:3957–3961.

Banting G, Ponnambalam S (1997) TGN38 and its orthologues: roles in post-TGN vesicle formation and maintenance of TGN morphology. Biochim Biophys Acta 1355:209–217.

Barrantes FJ (1993) Structural-functional correlates of the nicotinic acetylcholine receptor and its lipid microenvironment. FASEB J 7:1460–1467.

Barrantes FJ (2003) Transmembrane modulation of nicotinic acetylcholine receptor function. Curr Opin Drug Disc Dev 6:620–632.

Barrantes FJ, Antollini SS, Blanton MP, Prieto M (2000) Topography of nicotinic acetylcholine receptor membrane-embedded domains. J Biol Chem 275:37333–37339.

Blanton MP, Xie Y, Dangott LJ, Cohen JB (1999) The steroid promegestone is a noncompetitive antagonist of the *Torpedo* nicotinic acetylcholine receptor that interacts with the lipid-protein interface. Mol Pharmacol 55:269–278.

Blount P, Merlie JP (1988) Native folding of an acetylcholine receptor α subunit expressed in the absence of other receptor subunits. J Biol Chem 263:1072–1080.

Blount P, Merlie JP (1989) Molecular basis of the two nonequivalent ligand binding sites of the muscle nicotinic acetylcholine receptor. Neuron 3:349–357.

Blount P, Merlie JP (1991) Characterization of an adult muscle acetylcholine receptor subunit by expression in fibroblasts. J Biol Chem 266:14692–14696.

Bonini IC, Antollini SS, Gutiérrez-Merino C, Barrantes FJ (2002) Sphingomyelin composition and physical asymmetries in native acetylcholine receptor-rich membranes. Eur Biophys J 31:417–427.

Bock JB, Klumperman J, Davanger S, Scheller RH (1997) Syntaxin 6 functions in *trans*-Golgi network vesicle trafficking. Mol Biol Cell 8:1261–1271.

Brown DA, Rose JK (1992) Sorting of GPI-anchored proteins to glycolipid-enriched membrane subdomains during transport to the apical cell surface. Cell 68:533–544.

Brusés JL, Chauvet N, Rutishauser U (2001) Membrane lipid raft are necessary for the maintenance of the α7-nicotinic acetylcholine receptor in somatic spines of ciliary neurons. J Neurosci 21:504–512.

Chardin P, McCormick F (1999) Brefeldin A: the advantage of being uncompetitive. Cell 97:153–155.

Corbin J, Wang HH, Blanton MP (1998) Identifying the cholesterol binding domain in the nicotinic acetylcholine receptor with [^{125}I]-azido-cholesterol. Biochim Biophys Acta 11:65–74.

Criado M, Eibl H, Barrantes FJ (1982) Effects of lipids on acetylcholine receptor. Essential need of cholesterol for maintenance of agonist-induced state transitions in lipid vesicles. Biochemistry 21:3622–3629.

Criado M, Eibl H, Barrantes FJ (1984) Functional properties of the acetylcholine receptor incorporated in model lipid membranes: differential effects of chain length and head group of phospholipids on receptor affinity states and receptor-mediated ion translocation. J Biol Chem 259:9188–9198.

Dalziel AW, Rollins ES, McNamee MG (1980) The effect of cholesterol on agonist-induced flux in reconstituted acetylcholine receptor vesicles. FEBS Lett 122:193–198.

Dhanvantari S, Loh YP (2000) Lipid raft association of carboxypeptidase E is necessary for its function as a regulated secretory pathway sorting secretory pathway sorting receptor. J Biol Chem 275:29887–29893.

Ellena JF, Blazing MA, McNamee MG (1983) Lipid-protein interactions in reconstituted membranes containing acetylcholine receptor. Biochemistry 22:5523–5535.

Folch J, Lees M, Sloane-Stanley GM (1957) A simple method for the isolation and purification of total lipids from animal tissues. J Biol Chem 226:497–509.

Gelman MS, Chang W, Thomas DY, Bergeron JJ, Prives JM (1995) Role of the endoplasmic reticulum chaperone calnexin in subunit folding and assembly of nicotinic acetylcholine receptors. J Biol Chem 270:15085–15092.

Green WN, Claudio T (1993) Acetylcholine receptor assembly: subunit folding and oligomerization occur sequentially. Cell 74:57–69.

Gu Y, Ralston E, Murphy-Erdosh C, Black RA, Hall ZW (1989) Acetylcholine receptor in a C2 muscle cell variant is retained in the endoplasmic reticulum. J Cell Biol 109:729–738.

Gu Y, Franco A, Gardner PD, Lansman JB, Forsayeth JR, Hall ZW (1990) Properties of embryonic and adult muscle acetylcholine receptors transiently expressed in COS cells. Neuron 5:147–157.

Hanada K, Nishijima M, Kiso M, Hasegawa A, Fujita S, Ogawa T, Akamatsu Y (1992) Sphingolipids are essential for the growth of Chinese hamster ovary cells: restoration of the growth of a mutant defective in sphingoid base biosynthesis by exogenous sphingolipids. J Biol Chem 267:23527–23533.

Hannan LA, Edidin M (1996) Traffic, polarity, and detergent solubility of a glycosylphosphatidylinositol-anchored protein after LDL-deprivation of MDCK cells. J Cell Biol 133:1265–1276.

Hansen GH, Niels-Christiansen L-L, Thorsen E, Immerdal L, Danielsen EM (2000) Cholesterol depletion of enterocytes: effect on the Golgi complex and apical membrane trafficking. J Biol Chem 275:5136–5142.

Heino S, Lusa S, Somerharju P, Ehnholm C, Olkkonen VM, Ikonen E (2000) Dissecting the role of the Golgi complex and lipid rafts in biosynthetic transport of cholesterol to the cell surface. Proc Natl Acad Sci USA 97:8375–8380.

Keller P, Simons K (1998) Cholesterol is required for surface transport of influenza virus hemagglutinin. J Cell Biol 140:1357–1367.

Kurzchalia TV, Parton RG (1999) Membrane microdomains and caveolae. Curr Opin Cell Biol 11:424–431.

Lange Y, Ramos BV (1983) Analysis of the distribution of cholesterol in the intact cell. J Biol Chem 258:15130–15134.

Lippincott-Schwartz J, Yuan L, Tipper C, Amherdt M, Orci L, Klausner RD (1991) Brefeldin A's effects on endosomes, lysosomes, and the TGN suggest a general mechanism for regulating organelle structure and membrane traffic. Cell 67:601–616.

Lowry OH, Rosebrough NJ, Farr AL, Randall RJ (1951) A protein determination by the Folin-phenol reagent. J Biol Chem 193:265–275.

Lucocq JM, Berger EG, Warren G (1989) Mitotic Golgi fragments in HeLa cells and their role in the reassembly pathway. J Cell Biol 109:463–474.

Marchand S, Bignami F, Stetzkowski-Marden F, Cartaud J (2000) The myristoylated protein rapsyn is cotargeted with the nicotinic acetylcholine receptor to the postsynaptic membrane via the exocytic pathway. J Neurosci 20:521–528.

Marchand S, Devillers-Thiéry A, Pons E, Changeux J-P, Cartaud J (2002) Rapsyn escorts the nicotinic acetylcholine receptor along the exocytic pathway via association with lipid rafts. J Neurosci 22:8891–8901.

Marsh D, Barrantes FJ (1978) Immobilized lipid in acetylcholine receptor-rich membranes from *T. marmorata*. Proc Natl Acad Sci USA 75:4329–4333.

Marsh D, Watts A, Barrantes FJ (1981) Phospholipid chain immobilization and steroid rotational immobilization in acetylcholine receptor-rich membranes from *Torpedo marmorata*. Biochim Biophys Acta 645:97–101.

McNamee MG, Ellena JF, Dalziel AW (1982) Lipid-protein interactions in membranes containing the acetylcholine receptor. Biophys J 37:103–109.

Nilsson T, Pypaert M, Hoe MH, Slusarewicz P, Berger EG, Warren G (1993) Overlapping distribution of two glycosyltransferases in the Golgi apparatus of HeLa cells. J Cell Biol 120:5–13.

Patrick J, McMillan J, Wolfson H, O'Brien JC (1977) Acetylcholine receptor metabolism in a nonfusing muscle cell line. J Biol Chem 252:2143–2153.

Popot JL, Demel RA, Sobel A, Van Deenen LLM, Changeux JP (1978) Interaction of the acetylcholine (nicotinic) receptor protein from *Torpedo marmorata* electic organ with monolayers of pure lipids. Eur J Biochem 85:27–42.

Roccamo AM, Pediconi MF, Aztiria E, Zanello L, Wolstenholme A, Barrantes FJ (1999) Cell defective in sphingolipid biosynthesis express low amount of muscle nicotinic acetylcholine receptor. Eur J Neurosci 11:1615–1623.

Rosa P, Barr FA, Stinchcombe JC, Binacchi C, Huttner WB (1992) Brefeldin A inhibits the formation of constitutive secretory vesicles and immature secretory granules from the *trans*-Golgi network. Eur J Cell Biol 59:265–274.

Ross AF, Green WN, Hartman DS, Claudio T (1991) Efficiency of acetylcholine receptor subunit assembly and its regulation by cAMP. J Cell Biol 113:623–636.

Roth J, Berger EG (1982) Immunocytochemical localisation of galactosyltransferase in HeLa cells: codistribution with thiamine pyrophosphatase in trans-Golgi cisternae. J Cell Biol 93:223–229.

Rouser G, Fleicher S, Yamamoto A (1970) Two-dimensional thin layer chromatographic separation of polar lipids. Lipids 5:494–496.

Schindler H (1982) Methods for reconstituting receptors in planar membranes. Neurosci Res Prog Bull 20:295–299.

Schmidt J, Raftery MA (1973) A simple assay for the study of solubilized acetylcholine receptors. Anal Biochem 52:349–354.

Simons K, van Meer G (1988) Lipid sorting in epithelial cells. Biochemistry 27:6197–6202.

Simons K, Ikonen E (1997) Functional rafts in cell membranes. Nature 387:569–572.

Smart EJ, Ying Y, Donzell DC, Anderson RG (1996) A role for caveolin in transport of cholesterol from endoplasmic reticulum to plasma membrane. J Biol Chem 271:29427–29435.

Smith MM, Lindstrom J, Merlie JP (1987) Formation of the alpha-bungarotoxin binding site and assembly of the nicotinic acetylcholine receptor subunits occur in the endoplasmic reticulum. J Biol Chem 262:4367–4376.

Stüven E, Porat A, Shimron F, Fass E, Kaloyanova D, Brügger B, Wieland FT, Elazar Z, Helms JB (2003) Intra-Golgi protein transport depends on a cholesterol balance in the lipid membrane. J Biol Chem 278:53112–53122.

Vandenbulcke F, Nouel D, Vincent JP, Mazella J, Beaudet A (2000) Ligand-induced internalization of neurotensin in transfected COS-7 cells: differential intracellular trafficking of ligand and receptor. J Cell Sci 113:2963–2975.

van Meer G, Simons K (1988) Lipid polarity and sorting in epithelial cells. J Cell Biochem 36:51–58.

Wanamaker CP, Christianson JC, Green WN (2003) Regulation of nicotinic acetylcholine receptor assembly. Ann NY Acad Sci 998:66–80.

Wang Y, Thiele C, Huttner WB (2000) Cholesterol is required for the formation of regulated and constitutive secretory vesicles from the *trans*-Golgi network. Traffic 1:952–962.

Wang JM, Zhang L, Yao Y, Viroonchatapan N, Rothe E, Wang ZZ (2002) A transmembrane motif governs the surface trafficking of nicotinic acetylcholine receptors. Nat Neurosci 5:963–970.

Watson RT, Pessin JE (2000) Functional cooperation of two independent targeting domains in syntaxin 6 is required for its efficient localization in the *trans*-Golgi network of 3T3L1 adipocytes. J Biol Chem 275:1261–1268.

Xia W, Zhang J, Perez R, Koo EH, Selkoe DJ (1997) Interaction between amyloid precursor protein and presenilins in mammalian cells: implications for the pathogenesis of Alzheimer disease. Proc Natl Acad Sci USA 94:8208–8213.

Yamanaka K, Kigoshi S, Muramatzu I (1986) Muscarinic receptor subtipes in bovine adrenal medulla. Biochem Pharmacol 35:3151–3157.

Yeagle PL (1993) The biophysics and cell biology of cholesterol: an hypothesis for the essential role of cholesterol in mammalian cells. In: Cholesterol in membrane models (Fine Gold L, eds), pp 1–12. Boca Raton, Florida: CRC Press.

Zaal KJM, Smith C, Polishchuk RS, Altan N, Presley JF, Roberts TH, Siggia E, Phair RD, Lippincott-Schwartz J (1999) Golgi membranes are absorbed into and reemerge from the ER during mitosis. Cell 99:589–601.

Zhang CF, Dhanvantari S, Lou H, Loh YP (2003) Sorting of carboxypeptidase E to the regulated secretory pathway requires interaction of its transmembrane domain with lipid rafts. Biochem J 369:453–460.

(Accepted 4 June 2004)
(Available online 20 August 2004)